The structure and photoluminescence of ZnO films prepared by post-thermal annealing zinc-implanted silica

Y.X. Liu[a], Y.C. Liu[a,b,*], D.Z. Shen[a], G.Z. Zhong[a], X.W. Fan[a], X.G. Kong[a], R. Mu[c], D.O. Henderson[c]

[a] *Open Laboratory of Excited State Processes, Chinese Academy of Science, Changchun Institute of Optics, Fine Mechanics and Physics, Chinese Academy of Science, Changchun 130021, People's Republic of China*
[b] *The Institute of Theoretical Physics, Northeast Normal University, Changchun 130024, People's Republic of China*
[c] *Chemical Physics Laboratory, Department of Physics, Fisk University, Nashville, TN 37208, USA*

Abstract

High-quality ZnO films have been prepared by using zinc ion implantation into silica followed by post-thermal annealing in oxygen at 700°C for varying lengths of time. The dependence of the structure and photoluminescence of ZnO films on the annealing time has been investigated using X-ray diffraction and photoluminescence spectra. The X-ray photoelectron spectra were used to investigate the ZnO film formation process. As the annealing time increased to 2 h, ZnO film exhibited (0 0 2)-preferred orientation and an intense UV emission with a full width of 11 nm (96 meV) at half maximum positioned at ≈ 377 nm (3.29 eV) at room temperature. © 2002 Elsevier Science B.V. All rights reserved.

1. Introduction

ZnO is a versatile semiconductor material with a wide band gap (3.37 eV) and a large exciton binding energy (60 meV) at room temperature. Lately, it has attracted much more interest in the application of optoelectronic devices, due to the discovery of room-temperature lasing and the ZnO random laser [1,2]. Many different techniques, such as molecular beam epitaxy (MBE) [3], metal organic chemical vapor deposition [4], pulse laser deposition [5], sputtering [6], spray pyrolysis [7] and electrophoresis [8], have been used to prepare ZnO film. Segawa et al. [9] have reported that the (0 0 2)-preferred orientation of the nanocrystal in ZnO film strongly affects the threshold of the ultraviolet (UV) lasing. When the ZnO sample was excited parallel to *c*-axis, the threshold was low. Although some of the above techniques can fabricate ZnO film with the (0 0 2)-preferred

*Corresponding author. Open Laboratory of Excited State Processes, Chinese Academy of Science, Changchun Institute of Optics, Fine Mechanics and Physics, Chinese Academy of Science, Changchun 130021, People's Republic of China. Tel.: +86-0431-5937596; fax: +86-0431-5955378.

E-mail address: ycliu@nenu.edu.cn (Y.C. Liu).

orientation and the intense UV emission, ZnO samples can be stained by reaction gases and it is not easy to prepare the large-area-uniform ZnO film. Recently, Cho et al. [10] have reported the intense ultraviolet photoluminescence (PL) of polycrystalline ZnO thin film prepared by the thermal oxidization of metallic Zn films. However, they could not fabricate ZnO with a (0 0 2)-preferred orientation. Therefore, it is imperative to find an easy and clean method to prepare a large-area-uniform ZnO film with a (0 0 2)-preferred orientation and an intense UV emission.

Ion implantation can be considered as one of the most flexible and clean technique to obtain nanoparticles [11]. We implanted Zn, a metal with a low melting point, into optical-grade fused silica. The zinc-implanted silica was then thermally annealed at 700°C in oxygen ambient for various annealing times to obtain ZnO on a silica substrate.

2. Experiment details

Optical-grade fused silica (Corning 7940) was used as the matrix. Zn ions with an energy of 160 keV were injected into the matrix. The dose of implanted Zn was $3 \times 10^{17} \, cm^{-2}$. Based on Rutherford back scattering measurement followed by (the transport of ions in matter) TRIM simulations, the Zn ion distribution in silica substrate forms a nearly perfect Gaussian shape with the peak position at $(0.12 + 0.01) \, \mu m$ below the surface.

After ion implantation, the samples were annealed in a standard furnace using a quartz tube reactor. To obtain the large-area-uniform ZnO films, the samples were treated at 700°C in an ambient of oxygen, as given in Table 1.

Table 1
The annealing condition of the samples

Sample	Annealing temperature (°C)	Ambient	Annealing time (h)
IM4	As-implanted	—	0
IM5	700	O_2	1
IM6	700	O_2	2

The samples were characterized by X-ray diffraction (XRD) (D/max-rA Rigoku using Cu K_α, $\lambda = 1.5418 \, Å$). The micro-photoluminescence of the ZnO films was recorded using a JY UV-Lamb micro-Raman spectrometer in back scattering geometry configuration at room temperature. The excitation wavelength was the 325 nm line of an He–Cd laser. The excitation area and power were $6 \, \mu m^2$ and 45 mW, respectively. X-ray photo-electron spectra were used to determine the chemical bonding configurations. XPS data were recorded at around $1 \times 10^{-8} \, Torr$ using a VG ESCALAB MK II system. To obtain binding energies of the constituent elements, a binding energy of 284.6 eV for a C1s line from the residual carbon on the surface was used as a reference.

3. Results and discussion

Fig. 1 shows the $\theta - 2\theta$ XRD patterns of the zinc-implanted silica annealed at 700°C in oxygen for different annealing times. The as-implanted sample, IM4, displays Zn polycrystalline behavior with a (1 0 1)-preferred orientation. While the as-implanted sample was being annealed at 700°C in oxygen ambient for 1 h, some Zn atoms were
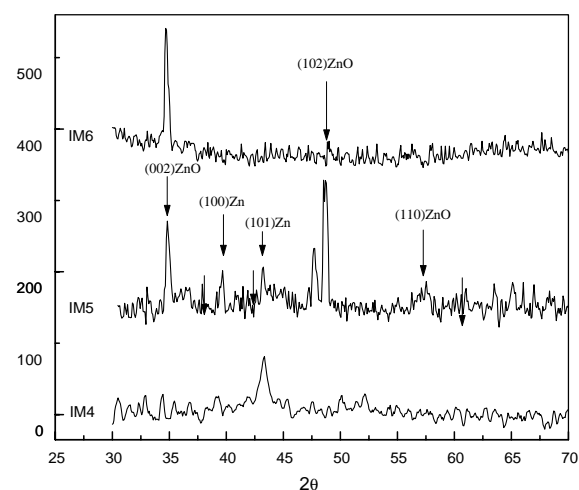
Fig. 1. XRD spectra of the samples IM4, IM5 and IM6. IM4: as-implanted sample; IM5: annealed at 700°C in O_2 for 1 h; IM6: annealed at 700°C in O_2 for 2 h.

oxidized from Zn to ZnO. Hence, IM5 displays both polycrystalline Zn and ZnO diffraction peaks. In this case, polycrystalline ZnO exhibits (0 0 2), (1 0 2) and (1 1 0) diffraction peaks. As the annealing time increases to 2 h, only one diffraction peak appears (at $2\theta = 34.43°$) which correspond to the (0 0 2) direction of the hexagonal ZnO structure. As the annealing time increases further, the (0 0 2) diffraction peak become sharper, due to the increased particle size as well as the enhanced degree of crystallization. These results indicated that Zn diffusion and the oxidation from Zn to ZnO occurred in the samples during the annealing processes.

XPS was used to identify ZnO oxidization during the annealing process for zinc-implanted silica under different annealing conditions. Fig. 2(a) shows a typical high-resolution XPS spectra from the Zn $2P_{3/2}$ core levels. The binding energy scale was calibrated using the C1s peak as reference energy (284.6 eV). According to the XRD results, the Zn $2P_{3/2}$ spectra of IM4, IM5 and IM6 can be described as the superposition of two component (Zn^0 and Zn^{+2}) peaks, corresponding to Zn atoms and ZnO whose binding energy are 1021.9 and 1022.5 eV, respectively [12]. In Fig. 2(a), we give the fitting results of the sample IM4. Fig. 2(b) shows the dependence of the integrated area under the Zn $2P_{3/2}$ peak and the percentage of oxidized Zn atoms of zinc-implanted silica on the annealing time in O_2 ambient. From Fig. 2(b), we find that the total integrated area of the Zn $2P_{3/2}$ peaks for the Zn and ZnO component and the percent of oxidized Zn atoms increase with increasing oxidation time. About 10% of Zn atoms were oxidized in the as-implanted sample. As the annealing time increased to 1 h, about 78% of Zn atoms were oxidized. As the annealing time increased to 2 h, about 93% of Zn atoms were oxidized. Because XPS is a sensitive surface probe and cannot give the information of Zn oxidization from the surface to inside, the surfaces of the samples IM4, IM5 and M6 were etched 15 min by Ar^+ ions sputtering. Thus, we obtained the similar results with the unetched samples. From a XPS analysis of the Si $2P_{3/2}$ core level, a decrease in the Si content on the silica surface as the annealing time increased was observed. Therefore, as the
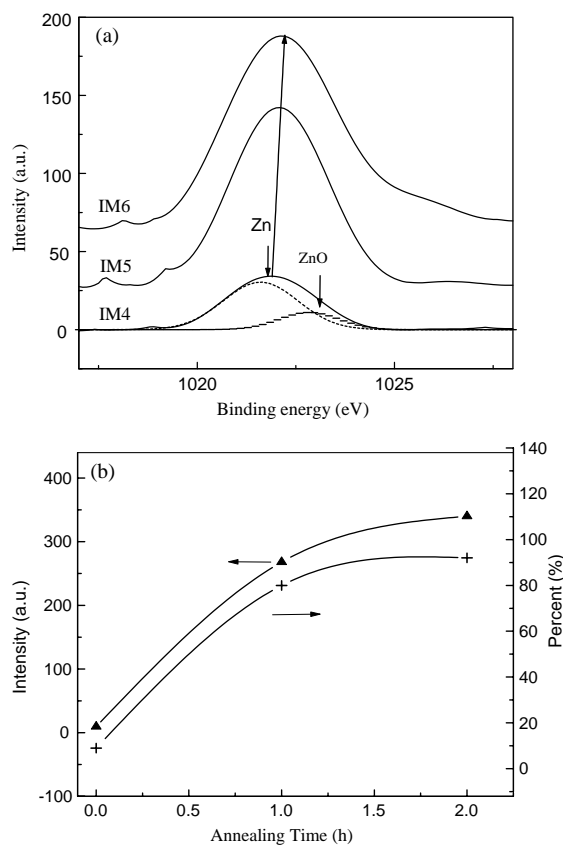
Fig. 2. (a) XPS spectra of Zn $2P_{3/2}$ peak for zinc-implanted silica under different annealing conditions. IM4: as-implanted sample; IM5: annealed at 700°C in O_2 for 1 h; IM6: annealed at 700°C in O_2 for 2 h. (b) The dependence of integrated area under the Zn $2P_{3/2}$ peak and the per cent of oxidized Zn atoms for zinc-implanted silica on the annealing time in O_2 ambient.

annealing time varied from 0 to 2 h in oxygen ambient, there was firstly Zn diffusion from inside the silica to the silica surface, followed by Zn nucleation and Zn oxidation on the silica surface and finally ZnO nanocrystals covered the whole silica surface. These results indicated ZnO formation on the silica surface.

Polycrystalline ZnO film consists of many small crystalline grains. To obtain the mean grain size of the samples, we adopted the Scherrer formula [13]:

$$D = \frac{0.9\lambda}{B \cos(\theta_B)},$$

where λ, θ_B and B are the X-ray wavelength (1.5418 Å), Bragg diffraction angle and full-width at half-maximum (FWHM) of the ZnO (0 0 2) diffraction peak near 34.42° or the Zn (1 0 1) diffraction peak near 43.3°, respectively. The mean grain size of Zn in IM4 is 10 nm. The mean grain sizes of the (0 0 2) orientated ZnO in IM5 and IM6 are 20 and 40 nm, respectively. Therefore, the quantum confinement effect can be observed in these samples.

To investigate the optical properties of ZnO film, a PL experiment was performed at room temperature. Fig. 3 shows the PL spectra of zinc-implanted silica annealed at 700°C under different annealing conditions. A significant PL peak was not observed in the as-implanted sample. As the annealing time increased to 1 h, PL with an intense ultraviolet near-band-edge emission around 377 nm (3.29 eV) and a very weak deep level emission in the range of 420–550 nm was observed. As the annealing time increased to 2 h, the ultraviolet emission around 377 nm was greatly enhanced.

To evaluate the quality of the ZnO films, the ratio R, defined as the intensity of the ultraviolet near-band-edge emission to the deep level emis-

Table 2
The dependence of the integrated intensity and FWHM of ultraviolet emission and the ratio R on the annealing time

Samples	The integrated intensity (a.u.)	FWHM (nm)	The ratio R
IM4	35	45	1
IM5	512	12.5	14
IM6	21,000	11 (96 meV)	40

sion, was used. The bigger the ratio R, the higher the quality of the ZnO film [14]. The inset in Fig. 3 gives the dependence of the normalized PL spectra on the annealing time. Table 2 shows the dependence of the integrated intensity, the FWHM of the ultraviolet emission and the ratio R on the annealing time. Table 2 shows that the integrated intensity of ultraviolet emission and the ratio R increase and the FWHM of ultraviolet emission decreases as the annealing time increases. These results show that the crystalline quality of the ZnO film improves as the annealing time increases. As shown in the inset of Fig. 3, a weak PL peak around 325 nm was observed in the IM5 sample. We can attribute this peak to the formation of small grain ZnO on the silica surface due to insufficient oxidization time. When the annealing time increased to 2 h, this peak disappeared since sufficient oxidization time allows for large grain formation of ZnO. The results obtained for sample IM6, given in Table 2, are comparable to the ratio R of 20 and FWHM of 114 meV at UV emission peak observed in MBE-grown ZnO thin films at room temperature [15].

The sharp UV emission peak around 3.29 eV presumably results from excitons. Due to the large exciton binding energy of ZnO (about 60 meV), excitons have been observed at room temperature. It has also been reported that thermal energy at room temperature may be enough to release bound excitons because the binding energy of the bound exciton is only a few millielectron volts [16]. The exciton level of our samples was 3.29 eV, blueshifted with respect to the typically reported free exciton peak position at 3.26 eV [15,17]. The above PL results are in good agreement with the XRD and XPS results.

Fig. 3. The PL spectra of zinc-implanted silica annealed at 700°C under the different annealing conditions. The inset gives the dependence of the normalized PL spectra of the samples on the annealing time. IM4: as-implanted sample; IM5: annealed at 700°C in O_2 for 1 h; IM6: annealed at 700°C in O_2 for 2 h.

4. Conclusions

We have fabricated high-quality ZnO thin films on a silica substrate by using ion implantation of zinc into silica followed by post-thermal annealing at 700°C in oxygen ambient under the different annealing condition. The XRD and XPS data show that ZnO film was formed on the silica surface. When the as-implanted sample was annealed at 700°C for 1 h, the mixed Zn and ZnO polycrystalline were observed and the UV emission around 377 nm was measured. As the annealing time increased to 2 h, ZnO film exhibited (0 0 2)-preferred orientation and the more intense UV emission with 11 nm (96 meV) around 377 nm (3.29 eV) at room temperature.

Acknowledgements

References

[1] Z.K. Tang, G.K.L. Wang, P. Yu, M. Kawaski, A. Ohtomo, H. Koinuma, Y. Segawa, Appl. Phys. Lett. 72 (1998) 3270.

[2] H. Cao, Y.G. Zhao, S.T. Ho, E.W. Seelig, Q.H. Wang, R.P.H. Chang, Phys. Rev. Lett. 82 (1999) 2278.

[3] Y. Chen, D.M. Bagnall, H.J. Koh, K.T. Park, K. Hiraga, Z. Zhu, T. Yao, J. Appl. Phys. 84 (1998) 3912.

[4] S. Bethke, H. Pan, B.W. Wesseis, Appl. Phys. Lett. 52 (1988) 138.

[5] R.D. Vispute, V. Talyansky, S. Choopun, R.P. Sharma, T. Venkatesan, M. He, X. Tang, J.B. Halpern, M.G. Spencer, Y.X. Li, K.A. Jones, Appl. Phys. Lett. 73 (1998) 348.

[6] H. Nanto, T. Minami, S. Takata, Phys. Stat. Sol. A 65 (1981) k131.

[7] F. Paraguay, D., W.L. Estrada, D.R. Acosta, N.E. Andrade, M. Miki-Yoshida, Thin Solid Films 350 (1999) 192.

[8] Sophie Peulon, Daniel Lincot, J. Electrochem. Soc. 145 (1998) 864.

[9] Y. Segawa, A. Ohtomo, M. Kawasaki, H. Koinuma, Z.K. Tang, P. Yu, G.K.L. Wong, Phys. Stat. Sol. B 202 (1997) 669.

[10] Sunglae Cho, Jing Ma, YunKi Kim, Yi Sun, George K.L. Wang, John B. Ketterson, Appl. Phys. Lett. 75 (1999) 2761.

[11] R. Mu, D.O. Henderson, Y.S. Tung, A. Ueda, C. Hall, W.E. Collins, C.W. White, R.A. Zuhr, Jane G. Zhu, J. Vac. Sci. Technol. A 14(3) (1996) 1482.

[12] S. Kohiki, T. Ohmura, K. Kusao, J. Electron Spectrosc. Relat. Phenom. 31 (1983) 85.

[13] B.D. Cullity, Elements of X-ray of Diffractions. Addition-Wesley, Reading MA (1978) P102.

[14] S. Bethke, H. Pan, B.W. Wessels, Appl. Phys. Lett. 52 (2) (1988) 138.

[15] Y. Chen, D.M. Bagnall, H.J. Koh, K.T. Park, K. Hiraga, Z. Zhu, T. Yao, J. Appl. Phys. 84 (1998) 3912.

[16] P. Zu, Z.K. Tang, G.K.L. Wong, M. Kawasaki, A. Ohtomo, H. Koinuma, Y. Segawa, Solid State Commun. 103 (1997) 459.

[17] D.M. Bagnall, Y.F. Chen, M.Y. Shen, Z. Zhu, T. Goto, T. Yao, J. Crystal Growth 184/185 (1998) 605.